



Research article

Imaging features of triple-negative breast cancers according to androgen receptor status



Rosalind P. Candelaria^{a,*}, Beatriz E. Adrada^a, Wei Wei^{b,1}, Alastair M. Thompson^{c,2},
Lumarie Santiago^a, Deanna L. Lane^a, Monica L. Huang^a, Elsa M. Arribas^a, Gaiane M. Rauch^a,
W. Fraser Symmans^d, Michael Z. Gilcrease^d, Lei Huo^d, Bora Lim^e, Naoto T. Ueno^e,
Stacy L. Moulder^{e,3}, Wei Tse Yang^{a,3}

^a Department of Diagnostic Radiology, Unit 1350, The University of Texas MD Anderson Cancer Center, 1515 Holcombe Boulevard, Houston, TX, 77030, USA

^b Department of Biostatistics, Unit 1411, The University of Texas MD Anderson Cancer Center, 1515 Holcombe Boulevard, Houston, TX, 77030, USA

^c Department of Breast Surgical Oncology, Unit 1434, The University of Texas MD Anderson Cancer Center, 1515 Holcombe Boulevard, Houston, TX, 77030, USA

^d Department of Pathology, Unit 085, The University of Texas MD Anderson Cancer Center, 1515 Holcombe Boulevard, Houston, TX, 77030, USA

^e Department of Breast Medical Oncology, Unit 1354, The University of Texas MD Anderson Cancer Center, 1515 Holcombe Boulevard, Houston, TX, 77030, USA

ARTICLE INFO

Keywords:

Triple-negative breast cancer
Androgen receptor
Mammography
Ultrasound
MRI

ABSTRACT

Objective: Different molecular subtypes of triple-negative breast cancer (TNBC) have previously been identified through analysis of gene expression profiles. The luminal androgen receptor (LAR) subtype has been shown to have a lower rate of pathologic complete response to neoadjuvant chemotherapy than other TNBC subtypes. The purpose of this study was to determine if the imaging features of TNBCs differ by AR (androgen receptor) status, which is a surrogate immunohistochemical (IHC) marker for the chemoresistant LAR subtype of TNBC.

Materials and methods: This sub-study was part of a clinical trial in patients with stage I-III TNBC who were prospectively monitored for response while receiving neoadjuvant systemic therapy (NAST) at a single comprehensive cancer center. This interim imaging analysis included 144 patients with known AR status measured by IHC. AR-positive (AR+) tumors were defined as those in which at least 10% of tumor cells had positive nuclear AR staining. Two experienced, fellowship-trained breast radiologists who were blinded to the IHC results retrospectively reviewed and reached consensus on all imaging studies for the index lesion (i.e., mammogram, ultrasound, and breast magnetic resonance imaging). The index lesion for each patient was reviewed and described according to the fifth edition of the Breast Imaging Reporting and Data System lexicon. Logistic regression modeling was used to identify imaging features predictive of AR status. $p \leq 0.05$ was considered statistically significant.

Results: Univariate logistic regression models for AR status showed that AR+ TNBC was significantly associated with heterogeneously dense breast composition on mammography ($p = 0.02$), mass with calcifications ($p = 0.05$), irregular mass shape on mammography ($p = 0.03$), and irregular mass shape on sonography ($p = 0.003$). Multivariate logistic regression models for AR status showed that AR+ TNBC was significantly associated with heterogeneously dense breast composition on mammography ($p = 0.01$), high mass density on mammography ($p = 0.003$), and irregular mass shape on sonography ($p = 0.0004$).

Conclusion: The imaging features of TNBCs differ by AR status. Multimodality breast imaging may help identify

Abbreviations: AR, androgen receptor; AR+, androgen receptor positive; AR-, androgen receptor negative; HER2, human epidermal growth factor receptor 2; IHC, immunohistochemical; LAR, luminal androgen receptor; MRI, magnetic resonance imaging; NAST, neoadjuvant systemic therapy; pCR, pathologic complete response; TNBC, triple-negative breast cancer

* Corresponding author.

E-mail addresses: rcandelaria@mdanderson.org (R.P. Candelaria), beatriz.adrada@mdanderson.org (B.E. Adrada), WWei@mdanderson.org, WEIW2@ccf.org (W. Wei), AThompson1@mdanderson.org, alastair.thompson@bcm.edu (A.M. Thompson), lumarie.santiago@mdanderson.org (L. Santiago), Deanna.Lane@mdanderson.org (D.L. Lane), mlhuang@mdanderson.org (M.L. Huang), earribas@mdanderson.org (E.M. Arribas), grauch@mdanderson.org (G.M. Rauch), fsymmans@mdanderson.org (W.F. Symmans), mgilcrease@mdanderson.org (M.Z. Gilcrease), LeiHuo@mdanderson.org (L. Huo), BLim@mdanderson.org (B. Lim), nueno@mdanderson.org (N.T. Ueno), smoulder@mdanderson.org (S.L. Moulder), wyang@mdanderson.org (W.T. Yang).

¹ Present address: Taussig Cancer Institute, Cleveland Clinic, 9500 Euclid Ave., Cleveland, OH, 44195, USA.

² Present address: Baylor College of Medicine, Division of Surgical Oncology, 6620 Main Street, Suite 1350, Houston, Texas, 77030, USA.

³ Co-senior authors.

<https://doi.org/10.1016/j.ejrad.2019.03.017>

Received 29 October 2018; Received in revised form 14 March 2019; Accepted 19 March 2019

0720-048X/© 2019 Elsevier B.V. All rights reserved.

the LAR subtype of TNBC, which has been shown to be a subtype that is relatively resistant to neoadjuvant chemotherapy.

1. Introduction

Triple-negative breast cancer (TNBC) comprises a heterogeneous collection of breast cancers that are grouped together because of a shared phenotype: lack of estrogen receptor (ER), progesterone receptor (PR), and human epidermal growth factor receptor 2 (HER2) expression. As a group, TNBCs are associated with poor prognosis with a higher risk of distant metastases and shorter overall survival when compared to the estrogen receptor positive or HER2 positive subtypes of breast cancer [1–7]. Furthermore, the approximately 50%–60% of patients with localized TNBC who have substantial residual disease at the time of surgery after completion of neoadjuvant systemic therapy (NAST) have an especially poor prognosis; more than 40–70% of them develop distant metastases within 5 years of their initial diagnosis [8–11]. There is currently no targeted therapy for TNBC. Novel targeted therapies are needed to improve the prognosis of patients with TNBC that is resistant to chemotherapy.

Gene expression profiling has identified several molecular subtypes of TNBC [12–15]. Notably in the analyses that have been reported in the literature to date, the luminal androgen receptor (LAR) subtype has consistently appeared [12–15], suggesting that the LAR subtype may be the most distinctive TNBC subtype. Retrospective evaluation of patients undergoing NAST has also shown that the LAR subtype is associated with lower rates of pathologic complete response (pCR) in comparison to other subtypes of TNBC, although the prognostic implication is presently less clear [9,12,13,16,17]. Nonetheless, TNBC cell lines with androgen receptor (AR) expression have been shown to respond to treatment with androgens and their antagonists [18,19]. Additionally, recent phase II clinical trials have shown promising results with AR inhibitors in patients with AR-positive (AR+) metastatic TNBC, further supporting therapeutic targeting of the AR signaling pathway [20,21].

Although gene expression profiling remains the gold standard for the molecular subtyping of breast cancer, gene expression profiling is not universally performed because it is time consuming and expensive. Currently, there are no commonly-used clinical assays that identify LAR TNBC by gene signature, and expression of AR by IHC is not routinely performed in patients receiving NAST. Imaging studies can help reveal which patients have chemoresistant TNBC and thereby prove valuable in decision making about which patients should be selected for evaluation for targeted therapy trials. Although TNBCs have classically been described as oval or round masses without calcifications and with circumscribed margins, many TNBC tumors do not exhibit these relatively benign imaging features [22–25]. The differences in the imaging presentation of TNBCs may align with differences in other features in this heterogeneous group of tumors comprising this clinical subtype for which no FDA-approved targeted therapy currently exists to enhance response to NAST. AR expression may shape the imaging appearances of TNBC tumors. Thus, the purpose of this study was to determine if the imaging features of TNBCs differ by AR status, which is a surrogate IHC marker for the chemoresistant LAR subtype of TNBC.

2. Materials and methods

2.1. Patient selection

This sub-study, which received approval from our institutional review board, is part of an ongoing clinical trial in patients with stage I-III TNBC who were prospectively monitored for response to NAST at a single comprehensive cancer center. All patients in the clinical trial gave informed consent before enrollment. The comprehensive list of

inclusion criteria and exclusion criteria for the two-armed, randomized clinical trial are available online (ClinicalTrials.gov identifier NCT02276443). This interim imaging analysis included 144 patients who were randomized to the clinical trial experimental arm of being informed of the results of molecular characterization of their tumor, including AR status; patients who were randomized to the clinical trial control arm in which molecular testing was not disclosed were not included in this analysis. The timeframe for this sub-study was December 2015 through July 2017.

2.2. Imaging

Two fellowship-trained breast radiologists with 8 years (RPC) and 13 years (BEA) of experience, respectively, retrospectively reviewed and reached consensus on all imaging studies (i.e., mammogram, ultrasound, and breast magnetic resonance imaging [MRI]) while blinded to the immunohistochemical results. The index lesion for each patient was reviewed and described according to the fifth edition of the Breast Imaging Reporting and Data System lexicon [26]. For patients with multiple foci of disease, the index lesion was defined as the dominant or largest tumor in the affected breast.

Three-view mammography (craniocaudal, mediolateral oblique, and lateromedial) was performed on all patients using digital mammography units (Hologic, Bedford, MA, USA). Breast composition was categorized as almost entirely fatty, scattered areas of fibroglandular density, heterogeneously dense, or extremely dense. Each index lesion was designated as a focal asymmetry, mass, or mass with calcifications. Masses were evaluated for shape, margin and density. Calcifications were evaluated for morphology and distribution.

Breast ultrasound was performed on all patients using Epiq 5G scanners with 12- to 18-MHz high frequency linear array transducers (Philips Healthcare, Andover, MA, USA). Transverse and longitudinal images of the index lesion were captured. Masses were evaluated for shape, margins, echo pattern, orientation and associated vascularity.

Table 1
Clinicopathologic characteristics in 144 patients with TNBC by AR status.

Characteristic	AR+ (n = 45)	AR- (n = 99)	p value
Age, mean (range), years	57 (28–77)	52 (26–77)	0.01
Tumor size, mean (range), cm	3.2 (1.1–11.9)	3.2 (1.4–10.2)	1.00
Tumor histology, n (%)			0.33
Ductal	40 (89)	81 (82)	
Lobular	1 (2)	1 (1)	
Metaplastic	4 (9)	17 (17)	
Histologic grade, n (%)			0.42
1	1 (2)	0 (0)	
2	8 (18)	12 (12)	
3	36 (80)	87 (88)	
Associated DCIS, n (%)			0.01
Yes	17 (38)	17 (17)	
No	28 (62)	82 (83)	
Ki-67 index, n (%)			0.003
High ($\geq 17\%$)	29 (64)	78 (79)	
Low ($< 17\%$)	6 (13)	1 (1)	
Unknown	10 (22)	20 (20)	
Axillary lymph node metastasis, n (%)			0.14
Yes	20 (44.4)	31 (31)	
No	25 (55.6)	68 (69)	

DCIS, ductal carcinoma in situ.

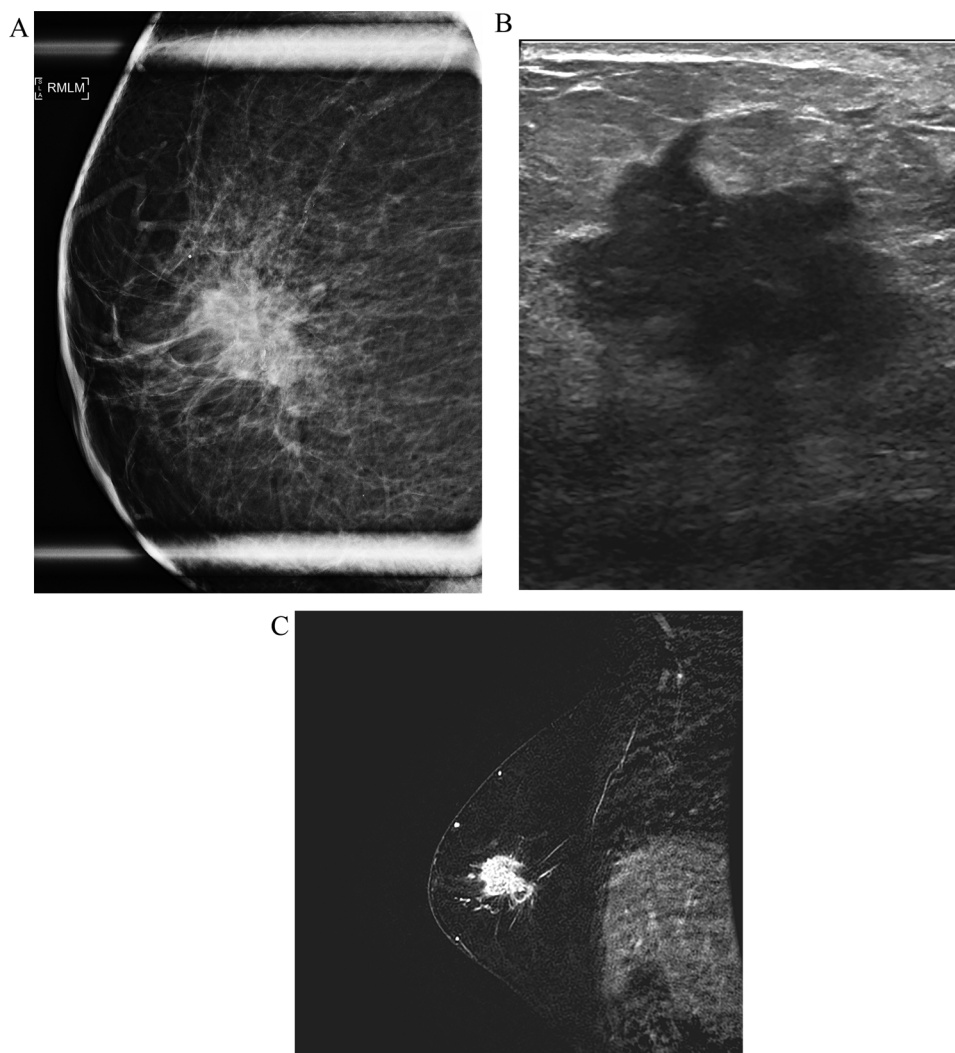


Fig. 1. 74-year-old woman with AR+ TNBC. (a) Right lateromedial magnification mammogram shows an irregular mass with associated coarse heterogeneous calcifications. (b) Breast ultrasound of the same mass shows irregular shape, angular margins, and a heterogeneous echo pattern. (c) Sagittal subtraction MR image of the same mass shows irregular shape and irregular margins.

Breast MRI was performed with patients in the prone position using a 3T scanner (GE Medical Systems, Milwaukee, WI, USA) with a dedicated 16-channel phased-array bilateral breast coil. The breast protocol consisted of bilateral axial T1-weighted sequence without fat suppression; axial or sagittal T2-weighted sequence with fat suppression; axial or sagittal dynamic contrast-enhanced image sets with fat suppression (a single unenhanced set followed by five postcontrast image sets) using the VIBRANT (GE Healthcare) acquisition technique before and five times after intravenous bolus injection of 0.1 mmol/kg of gadobenate dimeglumine (MultiHance, Bracco Imaging, Milan, Italy) or gadobutrol (Gadavist, Bayer HealthCare Pharmaceuticals, Leverkusen, Germany); and delayed axial contrast-enhanced three-dimensional fast spoiled gradient echo images with fat suppression. The amount of fibroglandular tissue and the background parenchymal enhancement were recorded for each patient. The index lesion was categorized as a mass or non-mass enhancement. Masses were evaluated for shape, margin, and internal enhancement characteristics. Non-mass enhancement was evaluated for distribution and internal enhancement pattern. A commercially available computer-aided detection system (DynaCAD version 2.0; Invivo, Gainesville, FL, USA) was used for kinetic curve assessment.

2.3. Immunohistochemistry

Tissue sections from 14-gauge core needle biopsy of the index lesion were subjected to immunohistochemistry staining and scoring by one of two experienced breast pathologists (MZG and LH). AR expression was quantified as the percentage of tumor cells with positive nuclear staining (0%–100%) using commercially available, standard CLIA-certified assays (clone AR 441, DAKO Corporation, Carpinteria, CA, USA). AR+ tumors were defined as those with at least 10% staining [27].

ER, PR, HER2, and Ki-67 data were extracted from pathology reports in the patients' electronic medical records. ER, PR, and Ki-67 were evaluated using immunohistochemical scoring as expressed as the percentage of cells with positive nuclear staining. ER+ and PR+ was defined as nuclear staining of $\geq 10\%$ [28]. HER2 status was determined by IHC or by fluorescence in situ hybridization (FISH); HER2+ was defined as 3+ by IHC or 2+ by IHC with FISH ratio of ≥ 2.0 for HER2:CEP17 (chromosome 17 centromere) or single probe copy number of ≥ 6 per cell [29]. Ki-67 expression was graded as high ($\geq 17\%$) or low ($< 17\%$) [30,31].

2.4. Data collection and statistical analysis

Patients' electronic medical records were reviewed to determine

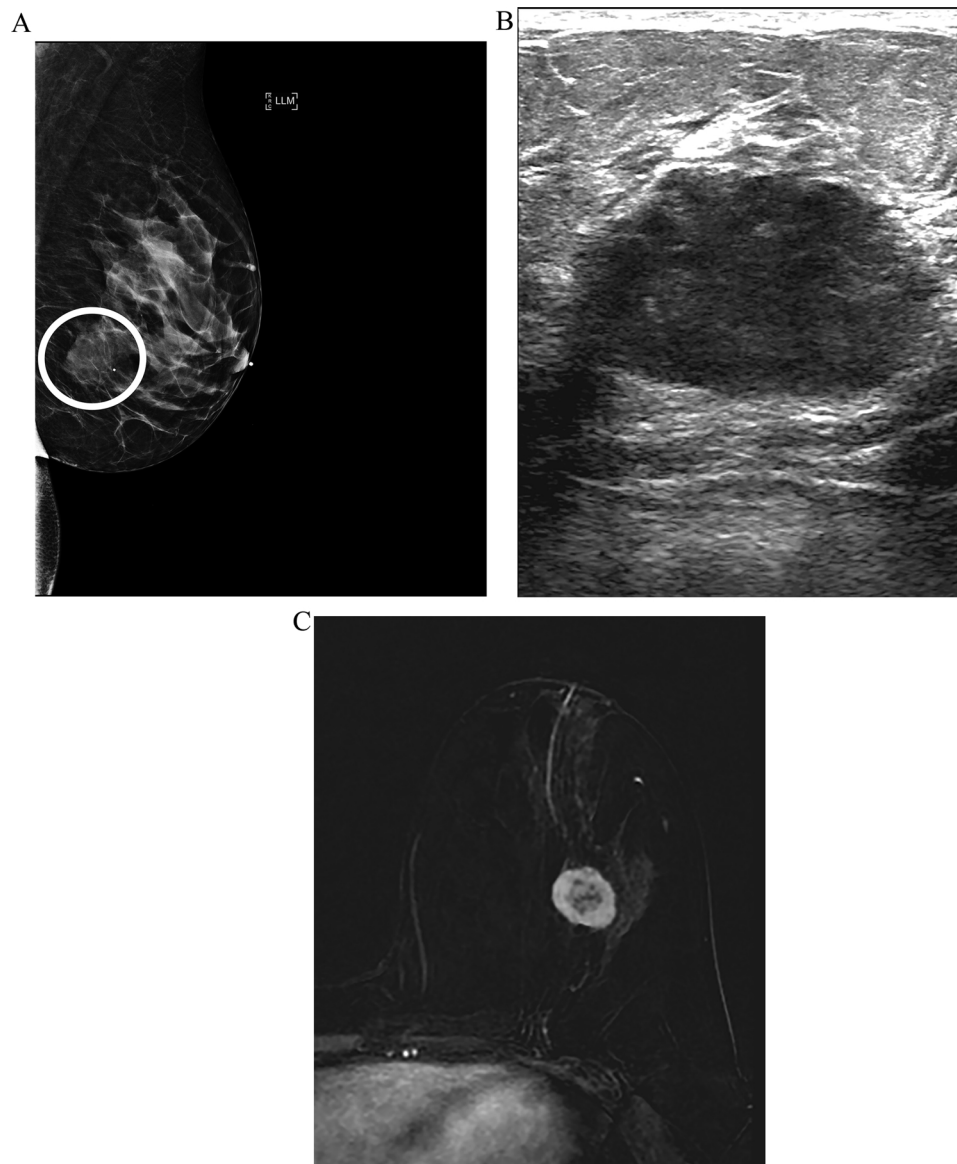


Fig. 2. 38-year-old woman with AR- TNBC. (a) Left lateromedial mammogram shows an oval mass (white circle) without calcifications and with circumscribed margins. (b) Breast ultrasound of the same mass shows oval shape, circumscribed margins, and hypoechoic echo pattern. (c) Axial subtraction MR image of the same mass shows oval shape, circumscribed margins, and heterogeneous internal enhancement.

age, tumor size, histology, grade, immunohistochemistry results, and axillary lymph node metastasis. A *t*-test was used to calculate the differences between means for patient age and tumor size in patients with AR+ versus AR- tumors. Fisher exact probability test was used to associate clinicopathologic characteristics with AR status. Logistic regression modeling was used to identify imaging features predictive of AR status. Univariate and multivariate models were fit to estimate odds ratios and 95% confidence intervals. Backwards elimination procedure was used to identify the final multivariate model for AR, starting with all imaging features in the model. Variables with smaller subsets were collapsed as follows for the logistic regression models: 1) breast composition on mammography: entirely fatty and scattered versus heterogeneously dense and extremely dense; 2) shape on ultrasound: round and oval versus irregular. All tests were two-sided, and *p* values of 0.05 or less were considered statistically significant. For factors with three or more levels, association with AR status was assessed by likelihood ratio test for its overall effect, resulting in an overall *p*-value. An overall *p*-value > 0.05 means that there was no significant difference between any pair of levels of that factor. Only factors with significant overall *p*-

values were assessed for pairwise *p*-values. Statistical analyses were performed using SAS version 9.4 (SAS Institute, Cary, NC, USA).

3. Results

3.1. Patient characteristics

Clinicopathologic characteristics are summarized in Table 1. Of the 144 patients in the study, 45 (31%) had AR+ tumors, and 99 (69%) had AR-negative (AR-) tumors. The mean age was 57 years for patients with AR+ TNBC (range, 28–77) and 52 years for patients with AR- TNBC (range, 26–77), *p* = 0.01. The mean tumor size was 3.2 cm in both groups (AR+ group range of 1.1 cm –11.9 cm and AR- group range of 1.4 cm –10.2 cm), *p* = 1.00. Examples of AR+ and AR- TNBCs are shown in Figs. 1 and 2, respectively. AR+ TNBC was more likely than AR- TNBC to have associated ductal carcinoma in situ described in the pathology report (38% [17/45] versus 17% [17/99], *p* = 0.01) and was less likely than AR- TNBC to have a high ($\geq 17\%$) Ki-67 index (64% [29/45] versus 79% [78/99], *p* = 0.003). All 144 patients

Table 2
Mammographic imaging features in 144 patients with TNBC by AR status.

Imaging feature	AR+ (n = 45)		AR- (n = 99)	
	N	(%)	N	(%)
Breast composition				
Almost entirely fatty	0	(0)	4	(4)
Extremely dense	0	(0)	4	(4)
Heterogeneously dense	35	(78)	53	(54)
Scattered areas of fibroglandular density	10	(22)	38	(38)
Lesion type				
Focal asymmetry ^a	2	(4)	1	(1)
Mass	28	(62)	80	(81)
Mass with calcifications	15	(33)	18	(18)
Mass shape^b				
Irregular	21	(49)	29	(30)
Oval	21	(49)	66	(67)
Round	1	(2)	3	(3)
Mass margin^b				
Circumscribed	5	(12)	6	(6)
Indistinct	3	(7)	20	(20)
Microlobulated	5	(12)	20	(20)
Obscured	21	(49)	42	(43)
Spiculated	9	(21)	10	(10)
Mass density^b				
Equal	4	(9)	23	(23)
High	39	(91)	75	(77)
Calcification morphology^c				
Amorphous	8	(47)	4	(22)
Coarse heterogeneous	4	(24)	8	(44)
Fine linear	0	(0)	2	(11)
Fine pleomorphic	5	(29)	4	(22)
Calcification distribution^c				
Grouped	15	(88)	16	(89)
Regional	1	(6)	0	(0)
Segmental	1	(6)	2	(11)

^a The two AR+ cases with focal asymmetry had associated calcifications. The AR- case with focal asymmetry did not have associated calcifications.

^b A denominator of 43 for the AR+ group and a denominator of 98 for the AR- group were used to calculate percentages.

^c A denominator of 17 for the AR+ group and a denominator of 18 for the AR- group were used to calculate percentages.

underwent mammography and sonography; 56 of the 144 (39%) patients underwent breast MRI.

3.2. Findings on mammography and sonography

Summary statistics of mammographic and ultrasound features by AR status are provided in [Tables 2 and 3](#), respectively; associations between these features and AR status were tested using logistic regression models, and p-values are listed in [Tables 4 and 5](#). Heterogeneously dense or extremely dense breasts were seen in 78% (35/45) of the patients with AR+ TNBC compared to 58% (57/99) of the patients with AR- TNBC. Mass with calcifications was the mammographic presentation in 33% (15/45) of the AR+ cases compared to 18% (18/99) of the AR- cases. AR+ tumors were more often irregular in shape than AR- tumors on mammography [49% (21/43) versus 30% (29/98)] and on sonography [51% (23/45) versus 25% (25/99)]. High density on mammography was seen in 91% (39/43) of the AR+ masses compared to 77% (75/98) of the AR- masses. Univariate logistic regression models for AR status showed that AR+ TNBC was significantly associated with heterogeneously dense breast composition on mammography ($p = 0.02$), mass with calcifications ($p = 0.05$), irregular mass shape on mammography ($p = 0.03$), and irregular mass shape on sonography ($p = 0.003$) ([Table 4](#)). Multivariate logistic regression models for AR status showed that AR+ TNBC was significantly associated with heterogeneously dense breast composition on mammography

Table 3
Ultrasound imaging features in 144 patients with TNBC by AR status.

Imaging feature	AR+ (n = 45)		AR- (n = 99)	
	N	(%)	N	(%)
Mass shape				
Irregular	23	(51)	25	(25)
Oval	22	(49)	73	(74)
Round	0	(0)	1	(1)
Mass margin				
Angular	2	(4)	2	(2)
Circumscribed	3	(7)	12	(12)
Indistinct	17	(38)	27	(27)
Microlobulated	21	(47)	55	(56)
Spiculated	2	(4)	3	(3)
Mass echo pattern				
Complex cystic and solid	9	(20)	24	(24)
Heterogeneous	14	(31)	24	(24)
Hypoechoic	22	(49)	51	(52)
Mass orientation				
Not parallel	10	(22)	16	(16)
Parallel	35	(78)	83	(84)
Vascularity				
Absent	15	(33)	28	(28)
Internal vascularity	24	(53)	55	(56)
Vessels in rim	6	(13)	16	(16)

($p = 0.01$), high mass density on mammography ($p = 0.003$), and irregular mass shape on sonography ($p = 0.0004$) ([Table 5](#)).

3.3. Breast MRI

MRI findings for the 56 patients (18/56 [32%] with AR+ TNBC and 38/56 [68%] with AR- TNBC) who had breast MRI are summarized in [Table 6](#). Logistic regression was not performed because of the small number of patients who had breast MRI. Nonetheless, a few trends were observed. Specifically, 87% (33/38) of the AR- TNBCs compared to 100% (18/18) of the AR+ TNBCs were masses, 76% (25/33) of the AR- masses versus 56% (10/18) of the AR+ masses were oval or round, and 51% (17/33) of the AR- masses compared to 84% (15/18) of the AR+ masses had noncircumscribed (i.e., irregular or spiculated) margins.

4. Discussion

The results of our study indicate that the imaging features of TNBCs differ based on AR status. Our findings revealed that AR+ TNBC was more likely than AR- TNBC to be found in breasts that were heterogeneously dense on mammography, to present as a mass with calcifications, to have high density on mammography, to have an irregular shape on mammography, and to have an irregular shape on sonography. These distinctive imaging features may aid in early identification of the LAR subtype of TNBC, which is driven by AR and has been shown to have a lower rate of pathologic complete response to neoadjuvant chemotherapy than other subtypes of TNBC [[9,12,13,16,17](#)]. Genomic profiling has identified the LAR subtype to be enriched in hormonally-regulated pathways, including expression of AR; therefore, AR expression, which can be assessed more readily based on IHC, may act as a surrogate for the LAR subtype of TNBC [[9,12,13,32](#)].

Our study validates the findings of Bae et al, who we believe are the only authors to date to report an association between AR expression and imaging characteristics in patients with TNBC [[33](#)]. The Bae et al cohort included 125 patients, 33 (26%) with AR+ and 92 (74%) with AR- TNBC, compared to our cohort of 144 patients (45 [31%] with AR+ and 99 [69%] with AR- TNBC) [[33](#)]. Bae et al concluded, as we did, that AR+ TNBC is associated with calcifications on mammography and

Table 4
Summary of univariate logistic regression model results for AR status.

Factor	Comparison	Odds ratio	95% LCL	95% UCL	Pairwise p value	Overall p value
Mammography breast composition	Heterogeneously dense/extremely dense vs. entirely fatty/scattered	2.58	1.18	6.03	0.02	
Mammography lesion type	Mass with calcifications vs. mass	0.44	0.20	1.00	0.05	
Mammography mass shape	Irregular vs. round/oval	2.27	1.09	4.78	0.03	
Mammography mass margin	Circumscribed vs. spiculated	0.93	0.20	4.15	NS	0.06
	Indistinct vs. spiculated	0.17	0.03	0.70	NS	
	Microlobulated vs. spiculated	0.28	0.07	1.02	NS	
	Obscured vs. spiculated	0.56	0.19	1.59	NS	
Mammography mass density	Equal vs. high	0.41	0.13	1.09	NS	
Ultrasound focality	Multifocal vs. unifocal	1.40	0.54	3.45	0.47	
Ultrasound mass shape	Irregular vs. round/oval	3.09	1.48	6.55	0.003	
Ultrasound mass margin	Angular vs. microlobulated	2.10	0.48	8.67	NS	0.36
	Circumscribed vs. microlobulated	0.65	0.14	2.31	NS	
	Indistinct vs. microlobulated	1.65	0.75	3.64	NS	
Ultrasound mass echo pattern	Complex cystic-solid vs. hypoechoic	0.87	0.34	2.13	NS	0.66
	Heterogeneous vs. hypoechoic	1.35	0.59	3.09	NS	
Ultrasound mass orientation	Not parallel vs. parallel	1.48	0.60	3.55	0.38	
Ultrasound vascularity	Absent vs. vessels in rim	1.43	0.47	4.67	NS	0.80
	Internal vascularity vs. vessels in rim	1.16	0.42	3.57	NS	

NS, not significant.

Table 5
Summary of multivariate logistic regression model results for AR status.

Factor	Comparison	Odds ratio	95% LCL	95% UCL	p value
Mammography breast composition	Heterogeneously dense/extremely dense vs. entirely fatty/scattered	3.27	1.36	7.86	0.01
Mammography mass density	High vs. equal	6.22	1.89	20.53	0.003
Ultrasound mass shape	Irregular vs. round/oval	4.71	2.00	11.09	0.0004

irregular shape on sonography [33]. All patients in the Bae et al cohort had breast MRI, and these authors further associated AR+ TNBC with non-enhancement on MRI [33]. However, we did not find an association between AR+ TNBC and non-enhancement on MRI, most likely because of the limited number of patients in our cohort who had breast MRI.

The difference in imaging profile between AR+ TNBC and AR–TNBC underscores their inherent biological differences. Our finding that AR+ cancers had a higher rate of associated ductal carcinoma in situ than AR– cancers helps to explain why AR+ cancers were more likely to present as a mass with calcifications on mammography. Additionally, the irregular shape of AR+ TNBC suggests that these tumors may be less proliferative, inciting a desmoplastic reaction from the surrounding tissue, in contrast to more aggressive tumors, which tend to be round/oval with circumscribed margins [34,35]. If AR+ tumors are indeed less proliferative, it is not surprising that the AR+ cancers in our cohort had lower Ki-67 expression than the AR–cancers, similar to the findings of Bae et al [33]. Although the LAR subtype has been shown to be less likely to achieve pCR from chemotherapy alone, the LAR subtype might still be a good prognostic marker and may be associated with improved survival [27,34–38]. However, there are conflicting reports regarding the prognosis of patients with the LAR subtype of TNBC [39,40], and further studies are required for clarification of the prognostic relevance of the LAR subtype within TNBC.

Studies have consistently shown that the LAR subtype of TNBC has a lower rate of pathologic complete response to neoadjuvant chemotherapy compared to the other subtypes of TNBC [9,12,13,16,17]. A potential advantage of identifying specific imaging features related to AR+ TNBC could be that such imaging surrogates may aid in the identification of subsets of patients with increased likelihood of chemoresistant disease, which can be confirmed with genomic profiling. Patients with confirmed LAR subtype of TNBC may be eligible for therapies targeting the AR signaling pathway.

Our single-center study has some limitations. First, we focused only on AR status and did not evaluate imaging features by genomic subtype;

imaging-specific features may differ even more by genomic subtype than by AR status. Second, the study is relatively small and warrants validation. Third, we did not evaluate interobserver variability but chose instead to use consensus decision making in the evaluation of the imaging features. Finally, the MRI-based findings must be interpreted with caution since these are observational findings due to the small sample size. We have revised our clinical trial design such that breast MRI is now required for all patients accrued to the trial. Continued tandem exploration of imaging features and genomic profiling may assist in development of improved targeted therapies for the different molecular subtypes of TNBC.

In conclusion, our study results suggest that the imaging features of TNBCs differ by AR status. Multimodality breast imaging may help identify the LAR subtype of TNBC, which has been shown to be a chemoresistant molecular subtype of TNBC.

Funding

This study was supported in part by the NIH/NCI under award number P30 CA016672, the MD Anderson Cancer Center Breast Cancer Moonshot Program and a CPRIT Multi-Investigator Research Award (MIRA): RP160710-C1-CPRIT.

IRB statement

This study was approved by the Institutional Review Board of The University of Texas MD Anderson Cancer Center (protocol 2014-0185; ClinicalTrials.gov Identifier NCT02276443).

Meeting presentation

Accepted for scientific oral presentation at the 2018 Radiological Society of North America Scientific Assembly and National Meeting, Chicago, Illinois.

Table 6
Breast MRI features in 56 patients with TNBC by AR status.

Imaging feature	AR+ (n = 18)		AR- (n = 38)	
	N	(%)	N	(%)
Amount of fibroglandular tissue				
Extremely fibroglandular	0	(0)	4	(11)
Heterogeneously fibroglandular	14	(78)	23	(61)
Scattered fibroglandular tissue	4	(22)	11	(29)
Background parenchymal enhancement				
Marked	1	(6)	1	(3)
Mild	6	(33)	19	(50)
Minimal	1	(6)	4	(11)
Moderate	10	(56)	14	(37)
Lesion type				
Non-mass enhancement	0	(0)	5	(13)
Mass	18	(100)	33	(87)
Mass shape^a				
Irregular	8	(44)	8	(24)
Oval	10	(56)	24	(73)
Round	0	(0)	1	(3)
Mass margin^a				
Circumscribed	3	(17)	16	(48)
Irregular	14	(78)	16	(48)
Spiculated	1	(6)	1	(3)
Mass internal enhancement characteristics^a				
Heterogeneous	14	(78)	20	(61)
Homogeneous	0	(0)	1	(3)
Rim enhancement	4	(22)	12	(36)
Non-mass enhancement distribution^b				
Linear	0	(0)	1	(20)
Multiple regions	0	(0)	3	(60)
Regional	0	(0)	1	(20)
Non-mass enhancement internal enhancement pattern^b				
Clumped	0	(0)	1	(20)
Heterogeneous	0	(0)	3	(60)
Homogeneous	0	(0)	1	(20)

^a A denominator of 18 for the AR+ group and a denominator of 33 for the AR- group were used to calculate percentages.

^b A denominator of 5 for the AR- group was used to calculate percentages.

Declaration of interests

Rosalind P. Candelaria, Beatriz E. Adrada, Wei Wei, Lumarie Santiago, Deanna L. Lane, Monica L. Huang, Elsa M. Arribas, Gaiane M. Rauch, Michael Z. Gilcrease, Lei Huo: Nothing to disclose.

W. Fraser Symmans: Delphi Diagnostics: intellectual property and founder shares; IONIS Pharmaceuticals: stock; Merck: advisory board honorarium; Almac Diagnostics: advisory board honorarium.

Alastair M. Thompson: Pfizer: honorarium.

Bora Lim: Pfizer: research funding.

Naoto T. Ueno: Pfizer: research funding; Epic Sciences: research funding.

Stacy L. Moulder: Oncothyreon: research funding and advisor; Seattle Genetics: research funding and advisor; Roche: research funding and advisor; Genentech: research funding and advisor; Novartis: research funding, advisor, and honorarium; Pfizer: research funding and advisor; EMD Serono: research funding and advisor; Bayer: advisor; Merck: advisor.

Wei Tse Yang: Wolters Kluwer: consultant; GE Healthcare: consultant; Seno Medical Instruments: advisory committee member; Elsevier: royalties.

Acknowledgements

Stephanie Deming, Rebekah Gould, Alyson Clayborn, Thorunn Helgason, Lisa Ravenberg.

References

- [1] L.A. Carey, C.M. Perou, C.A. Livasy, L.G. Dressler, D. Cowan, K. Conway, G. Karaca, M.A. Troester, C.K. Tse, S. Edmiston, S.L. Deming, J. Geradts, M.D. Cheang, T.O. Nielsen, P.G. Moorman, H.S. Earp, R.C. Millikan, Race, breast cancer subtypes, and survival in the Carolina Breast Cancer Study, *JAMA* 295 (2006) 2492–2502.
- [2] R. Dent, M. Trudeau, K.I. Pritchard, W.M. Hanna, H.K. Kahn, C.A. Sawka, L.A. Lickley, E. Rawlinson, P. Sun, S.A. Narod, Triple-negative breast cancer: clinical features and patterns of recurrence, *Clin. Cancer Res.* 13 (15 Pt 1) (2007) 4429–4434.
- [3] Early Breast Cancer Trialists' Collaborative Group (EBCTCG), Effects of chemotherapy and hormonal therapy for early breast cancer on recurrence and -year survival: an overview of the randomised trials, *Lancet* 365 (9472) (2005) 1687–1717.
- [4] B.G. Haffty, Q. Yang, M. Reiss, T. Kearney, S.A. Higgins, J. Weidhaas, L. Harris, W. Hait, D. Toppmeyer, Locoregional relapse and distant metastasis in conservatively managed triple negative early-stage breast cancer, *J. Clin. Oncol.* 24 (36) (2006) 5652–5657.
- [5] T. Miyake, T. Nakayama, Y. Naoi, N. Yamamoto, Y. Otani, S.J. Kim, K. Shimazu, A. Shimomura, N. Maruyama, Y. Tamaki, S. Noguchi, GSTP1 expression predicts poor pathological complete response to neoadjuvant chemotherapy in ER-negative breast cancer, *Cancer Sci.* 103 (5) (2012) 913–920.
- [6] T. Ovarcicak, S.G. Frkovic, E. Matos, B. Mozina, S. Borstnar, Triple negative breast cancer - prognostic factors and survival, *Radiol. Oncol.* 45 (1) (2011) 46–52.
- [7] S.K. Pal, B.H. Childs, M. Pegram, Triple negative breast cancer: unmet medical needs, *Breast Cancer Res. Treat.* 125 (3) (2011) 627–636.
- [8] C. Liedtke, C. Mazouni, K.R. Hess, F. André, A. Tordai, J.A. Mejia, W.F. Symmans, A.M. Gonzalez-Angulo, B. Hennessy, M. Green, M. Cristofanilli, G.N. Hortobagyi, L. Pusztai, Response to neoadjuvant therapy and long-term survival in patients with triple-negative breast cancer, *J. Clin. Oncol.* 26 (8) (2008) 1275–1281.
- [9] H. Masuda, K.A. Baggerly, Y. Wang, Y. Zhang, A.M. Gonzalez-Angulo, F. Meric-Bernstam, V. Valero, B.D. Lehmann, J.A. Pietenpol, G.N. Hortobagyi, W.F. Symmans, N.T. Ueno, Differential response to neoadjuvant chemotherapy among 7 triple-negative breast cancer molecular subtypes, *Clin. Cancer Res.* 19 (19) (2013) 5533–5540.
- [10] W.F. Symmans, C. Wei, R. Gould, X. Yu, Y. Zhang, M. Liu, A. Walls, A. Bousamra, M. Ramineni, B. Sinn, K. Hunt, T.A. Buchholz, V. Valero, A.U. Buzdar, W. Yang, A.M. Brewster, S. Moulder, L. Pusztai, C. Hatzis, G.N. Hortobagyi, Long-term prognostic risk after neoadjuvant chemotherapy associated with residual cancer burden and breast cancer subtype, *J. Clin. Oncol.* 35 (10) (2017) 1049–1060.
- [11] P. Sharma, S. López-Tarruella, J.A. García-Saenz, Q.J. Khan, H.L. Gómez, A. Prat, F. Moreno, Y. Jerez-Gilarranz, A. Barnadas, A.C. Picornell, M. Del Monte-Millán, M. González-Rivera, T. Massarrah, B. Pelaez-Lorenzo, M.I. Palomero, R. González Del Val, J. Cortés, H. Fuentes-Rivera, D.B. Morales, I. Márquez-Rodas, C.M. Perou, C. Lehn, Y.Y. Wang, J.R. Klemp, J.V. Mammen, J.L. Wagner, A.L. Amin, A.P. O'Dea, J. Heldstab, R.A. Jensen, B.F. Kimler, A.K. Godwin, M. Martín, Pathological response and survival in triple-negative breast cancer following neoadjuvant carboplatin plus docetaxel, *Clin. Cancer Res.* (July) (2018), <https://doi.org/10.1158/1078-0432.CCR-18-0585> [Epub ahead of print].
- [12] B.D. Lehmann, J.A. Bauer, X. Chen, M.E. Sanders, A.B. Chakravarthy, Y. Shyr, J.A. Pietenpol, Identification of human triple-negative breast cancer subtypes and preclinical models for selection of targeted therapies, *J. Clin. Invest.* 121 (7) (2011) 2750–2767.
- [13] B.D. Lehmann, B. Jovanović, X. Chen, M.V. Estrada, K.N. Johnson, Y. Shyr, H.L. Moses, M.E. Sanders, J.A. Pietenpol, Refinement of triple-negative breast cancer molecular subtypes: implications for neoadjuvant chemotherapy selection, *PLoS One* 11 (6) (2016) e0157368, <https://doi.org/10.1371/journal.pone.0157368>.
- [14] M.D. Burstein, A. Tsimelzon, G.M. Poage, K.R. Covington, A. Contreras, S.A. Fuqua, M.I. Savage, C.K. Osborne, S.G. Hilsenbeck, J.C. Chang, G.B. Mills, C.C. Lau, P.H. Brown, Comprehensive genomic analysis identifies novel subtypes and targets of triple-negative breast cancer, *Clin. Cancer Res.* 21 (7) (2015) 1688–1698.
- [15] Y.R. Liu, Y.Z. Jiang, X.E. Xu, K.D. Yu, X. Jin, X. Hu, W.J. Zuo, S. Hao, J. Wu, G.Y. Liu, G.H. Di, D.Q. Li, X.H. He, W.G. Hu, Z.M. Shao, Comprehensive transcriptome analysis identifies novel molecular subtypes and subtype-specific RNAs of triple negative breast cancer, *Breast Cancer Res.* 15 (2016) 18–33.
- [16] I. Echavarría, S. López-Tarruella, A. Picornell, J.A. García-Saenz, Y. Jerez, K. Hoadley, H.L. Gómez, F. Moreno, M.D. Monte-Millán, I. Márquez-Rodas, E. Alvarez, R. Ramos-Medina, J. Gayarré, T. Massarrah, I. Ocaña, M. Cebollero, H. Fuentes, A. Barnadas, A.I. Ballesteros, U. Bohn, C.M. Perou, M. Martín, Pathological response in a triple-negative breast cancer cohort treated with neoadjuvant carboplatin and docetaxel according to Lehmann's refined classification, *Clin. Cancer Res.* 24 (8) (2018) 1845–1852.
- [17] A. Santonja, A. Sánchez-Muñoz, A. Lluch, M.R. Chica-Parrado, J. Albanell, J.I. Chacón, S. Antolín, J.M. Jerez, J. de la Haba, V. de Luque, C.E. Fernández-De Sousa, L. Vicioso, Y. Plata, C.L. Ramírez-Tortosa, M. Álvarez, C. Llácer, I. Zarcos-Pedrinaci, E. Carrasco, R. Caballero, M. Martín, E. Alba, Triple negative breast cancer subtypes and pathologic complete response rate to neoadjuvant chemotherapy, *Oncotarget* 9 (41) (2018) 26406–26416.
- [18] M. Ni, Y. Chen, E. Lim, H. Wimberly, S.T. Bailey, Y. Imai, D.L. Rimm, X.S. Liu, M. Brown, Targeting androgen receptor in estrogen receptor-negative breast cancer, *Cancer Cell* 20 (1) (2011) 119–131.
- [19] R. Huang, J. Han, X. Liang, S. Sun, Y. Jiang, B. Xia, M. Niu, D. Li, J. Zhang, S. Wang, W. Wei, Q. Liu, W. Zheng, G. Zhang, Y. Song, D. Panga, Androgen receptor expression and bicalutamide antagonize androgen receptor inhibit β -catenin

- transcription complex in estrogen receptor-negative breast cancer, *Cell. Physiol. Biochem.* 43 (6) (2017) 2212–2225.
- [20] A. Gucalp, T.A. Traina, Triple-negative breast cancer: role of the androgenreceptor, *Cancer J.* 16 (1) (2010) 62–65, <https://doi.org/10.1097/PP0.0b013e3181ce4ae1> Review. Erratum in: *Cancer J.* 16(6) (2010) 643.
- [21] A. Gucalp, S. Tolane, S.J. Isakoff, J.N. Ingle, M.C. Liu, L.A. Carey, K. Blackwell, H. Rugo, L. Nabell, A. Forero, V. Stearns, A.S. Doane, M. Danso, M.E. Moynahan, L.F. Momen, J.M. Gonzalez, A. Akhtar, D.D. Giri, S. Patil, K.N. Feigin, C.A. Hudis, T.A. Traina, Translational Breast Cancer Research Consortium (TBCRC 011), phase II trial of bicalutamide in patients with androgen receptor-positive, estrogen receptor-negative metastatic breast cancer, *Clin. Cancer Res.* 19 (2013) 5505–5512.
- [22] M. Boissarie-Lacroix, G. Macgrogan, M. Debled, S. Ferron, M. Asad-Syed, P. McKelvie-Sebileau, S. Mathoulin-Pélessier, V. Brouste, G. Hurtevent-Labrot, Triple-negative breast cancers: associations between imaging and pathological findings for triple-negative tumors compared with hormone receptor-positive/human epidermal growth factor receptor-2-negative breast cancers, *Oncologist* 18 (7) (2013) 802–811.
- [23] B.E. Dogan, A.M. Gonzalez-Angulo, M. Gilcrease, M.J. Dryden, W.T. Yang, Multimodality imaging of triple receptor-negative tumors with mammography, ultrasound, and MRI, *Am. J. Roentgenol.* 194 (2010) 1160–1166.
- [24] E.S. Ko, B.H. Lee, H.A. Kim, W.C. Noh, M.S. Kim, S.A. Lee, Triple-negative breast cancer: correlation between imaging and pathological findings, *Eur. Radiol.* 20 (5) (2010) 1111–1117.
- [25] K.M. Krizmanich-Conniff, C. Paramagul, S.K. Patterson, M.A. Helvie, M.A. Roubidoux, J.D. Myles, K. Jiang, M. Sabel, Triple receptor-negative breast cancer: imaging and clinical characteristics, *AJR Am. J. Roentgenol.* 199 (2012) 458–464.
- [26] American College of Radiology ACR BI-RADS Atlas: Breast Imaging Reporting and Data System, fifth ed., (2013) Reston, Virginia.
- [27] F.E. Vera-Badillo, A.J. Templeton, P. de Gouveia, I. Diaz-Padilla, P.L. Bedard, M. Al-Mubarak, B. Seruga, I.F. Tannock, A. Ocana, E. Amir, Androgen receptor expression and outcomes in early breast cancer: a systematic review and meta-analysis, *J. Natl. Cancer Inst.* 106 (1) (2014), <https://doi.org/10.1093/jnci/djt319>.
- [28] M.E. Hammond, D.F. Hayes, M. Dowsett, D.C. Allred, K.L. Hagerty, S. Badve, P.L. Fitzgibbons, G. Francis, N.S. Goldstein, M. Hayes, D.G. Hicks, S. Lester, R. Love, P.B. Mangu, L. McShane, K. Miller, C.K. Osborne, S. Paik, J. Perlmutter, A. Rhodes, H. Sasano, J.N. Schwartz, F.C. Sweep, S. Taube, E.E. Torlakovic, P. Valenstein, G. Viale, D. Visscher, T. Wheeler, R.B. Williams, J.L. Wittliff, A.C. Wolff, American Society of Clinical Oncology/College of American Pathologists guideline recommendations for immunohistochemical testing of estrogen and progesterone receptors in breast cancer, *Arch. Pathol. Lab. Med.* 134 (6) (2010) 907–922.
- [29] A.C. Wolff, M.E. Hammond, D.G. Hicks, M. Dowsett, L.M. McShane, K.H. Allison, D.C. Allred, J.M. Bartlett, M. Bilous, P. Fitzgibbons, W. Hanna, R.B. Jenkins, P.B. Mangu, S. Paik, E.A. Perez, M.F. Press, P.A. Spears, G.H. Vance, G. Viale, D.F. Hayes, Recommendations for human epidermal growth factor receptor 2 testing in breast cancer: American Society of Clinical Oncology/College of American Pathologists clinical practice guideline update, *Arch. Pathol. Lab. Med.* 138 (2014) 241–256.
- [30] S.E. Pinder, P. Wencyk, D.M. Sibbering, J.A. Bell, C.W. Elston, R. Nicholson, J.F. Robertson, R.W. Blamey, I.O. Ellis, Assessment of the new proliferation marker MIB1 inbreast carcinoma using image analysis: associations with other prognostic factors and survival, *Br. J. Cancer* 71 (1) (1995) 146–149.
- [31] M. Dowsett, T.O. Nielsen, R. A'Hern, J. Bartlett, R.C. Coombes, J. Cuzick, M. Ellis, N.L. Henry, J.C. Hugh, T. Lively, L. McShane, S. Paik, F. Penault-Llorca, L. Prudkin, M. Regan, J. Salter, C. Sotiriou, I.E. Smith, G. Viale, J.A. Zujewski, D.F. Hayes, International Ki-67 in Breast Cancer Working Group. Assessment of Ki67 in breast cancer: recommendations from the international Ki67 in Breast Cancer Working Group, *J. Natl. Cancer Inst.* 103 (22) (2011) 1656–1664.
- [32] L. Gerratana, D. Basile, G. Buono, S. De Placido, M. Giuliano, S. Minichillo, A. Coinu, F. Martorana, I. De Santo, L. Del Mastro, M. De Laurentiis, F. Puglisi, G. Arpino, Androgen receptor in triple negative breast cancer: a potential target for the targetless subtype, *Cancer Treat. Rev.* 68 (2018) 102–110.
- [33] M.S. Bae, S.Y. Park, S.E. Song, W.H. Kim, S.H. Lee, W. Han, I.A. Park, D.Y. Noh, W.K. Moon, Heterogeneity of triple-negative breast cancer: mammographic, US, and MR imaging features according to androgen receptor expression, *Eur. Radiol.* 25 (2) (2015) 419–427.
- [34] Q. Qu, Y. Mao, X.C. Fei, K.W. Shen, The impact of androgen receptor expression on breast cancer survival: a retrospective study and meta-analysis, *PLoS One* 8 (12) (2013) e82650, <https://doi.org/10.1371/journal.pone.0082650>.
- [35] K.D. Yu, R. Zhu, M. Zhan, A.A. Rodriguez, W. Yang, S. Wong, A. Makris, B.D. Lehmann, X. Chen, I. Mayer, J.A. Pietenpol, Z.M. Shao, W.F. Symmans, J.C. Chang, Identification of prognosis-relevant subgroups in patients with chemoresistant triple-negative breast cancer, *Clin. Cancer Res.* 19 (2013) 2723–2733.
- [36] K.M. McNamara, T. Yoda, Y. Miki, N. Chanplakorn, S. Wongwaisayawan, P. Incharoen, Y. Kongdan, L. Wang, K. Takagi, T. Mayu, Y. Nakamura, T. Suzuki, N. Nemoto, M. Miyashita, K. Tamaki, T. Ishida, N. Ohuchi, H. Sasano, Androgenic pathway in triple negative invasive ductal tumors: its correlation with tumor cell proliferation, *Cancer Sci.* 104 (2013) 639–646.
- [37] S. Loibl, B.M. Müller, G. von Minckwitz, M. Schwabe, M. Roller, S. Darb-Esfahani, B. Ataseven, A. du Bois, A. Fissler-Eckhoff, B. Gerber, U. Kulmer, J.U. Alles, K. Mehta, C. Denkert, Androgen receptor expression in primary breast cancer and its predictive and prognostic value in patients treated with neoadjuvant chemotherapy, *Breast Cancer Res. Treat.* 130 (2) (2011) 477–487.
- [38] P. Gasparini, M. Fassan, L. Cascione, G. Guler, S. Balci, C. Irkkan, C. Paisie, F. Lovat, C. Morrison, J. Zhang, A. Scarpa, C.M. Croce, C.L. Shapiro, K. Huebner, Androgen receptor status is a prognostic marker in non-basal triple negative breast cancers and determines novel therapeutic options, *PLoS One* 9 (2) (2014) e88525.
- [39] J.E. Choi, S.H. Kang, S.J. Lee, Y.K. Bae, Androgen receptor expression predicts decreased survival in early stage triple-negative breast cancer, *Ann. Surg. Oncol.* 1(1) (2015) 82–89.
- [40] L.J. McGhan, A.E. McCullough, C.A. Protheroe, A.C. Dueck, J.J. Lee, R. Nunez-Nateras, E.P. Castle, R.J. Gray, N. Wasif, M.P. Goetz, J.R. Hawse, T.J. Henry, M.T. Barrett, H.E. Cunliffe, B.A. Pockaj, Androgen receptor-positive triple negative breast cancer: a unique breast cancer subtype, *Ann. Surg. Oncol.* 21 (2) (2014) 361–367.